# Sea-ice change and its connection with climate change in the Arctic in CMIP2 simulations

Zeng-Zhen Hu,[1] Svetlana I. Kuzmina,[2] Lennart Bengtsson,[3,4] and David M. Holland[5]

Received 16 December 2003; revised 1 March 2004; accepted 13 April 2004; published 22 May 2004.

[1] In this work, we analyze the two-dimensional distribution of mean and intermodel spread of Arctic sea ice and climate change at the time of $CO_2$ doubling and their connection using the simulations from the second phase of the Coupled Model Intercomparison Project (CMIP2). Arctic surface warming at the time of $CO_2$ doubling is found to be not evenly distributed and ranges from 1° to 5°C. The intermodel spread is pronounced in the Arctic Ocean, particularly in the Barents Sea. Reduction of sea-ice thickness (SIT) is in the range 0.3–1.8 m and mainly appears in the Greenland-Barents Seas. Meanwhile, sea-ice concentrations (SIC) decrease more than 10% in most regions of the Arctic Ocean. The sensitivity of Arctic surface air temperature change with respect to sea-ice area change is model-dependent. For some models, the sensitivity is different even in different periods of the transient integration. Values of the sensitivity vary from $-2.0$ to $-0.5$°C/$10^6$ km$^2$ for most CMIP2 models. A colder (warmer) Arctic climate may favor a higher (lower) sensitivity. The simulated mean and intermodel spread patterns of surface air temperature (SAT) change are similar to those of SIT and sea level pressure (SLP) changes. This implies that the mean and intermodel spread of projected Arctic climate change are influenced by the interaction between sea ice and the atmosphere. Both SIT and SIC are sensitive to the increase in greenhouse gas concentrations, and are connected with SAT and SLP changes in the Arctic. The average of all model simulations indicates that the north-south SLP gradient and the mean westerly winds are enhanced by $CO_2$ doubling. Finally, both the mean and intermodel spread patterns show considerable differences between models with and without flux adjustment in some regions. *INDEX TERMS:* 1620 Global Change: Climate dynamics (3309); 1854 Hydrology: Precipitation (3354); 3349 Meteorology and Atmospheric Dynamics: Polar meteorology; 3309 Meteorology and Atmospheric Dynamics: Climatology (1620); *KEYWORDS:* Arctic sea ice, global warming, CMIP2 simulations

**Citation:** Hu, Z.-Z., S. I. Kuzmina, L. Bengtsson, and D. M. Holland (2004), Sea-ice change and its connection with climate change in the Arctic in CMIP2 simulations, *J. Geophys. Res.*, *109*, D10106, doi:10.1029/2003JD004454.

## 1. Introduction

[2] As an integral part of the global climate system, the Arctic has experienced significant change in recent decades [*Johannessen et al.*, 1995, 1999; *Rothrock et al.*, 1999; *Vinnikov et al.*, 1999]. The following is some evidence mentioned in the recent *Intergovernmental Panel on Climate Change* (*IPCC*) [2001] report. Under a background of 0.4–0.6°C increase of global-averaged temperature in the 20th century, Northern Hemisphere (NH) spring and summer sea-ice extent has decreased by about 10 to 15% since the 1950s. The influence of human activities on the observed sea-ice changes has been recognized by some model investigations. For example, ensemble simulations of HadCM3 coupled general circulation model (CGCM) demonstrated that internal variability and natural forcing (solar and volcanic) of the climate system are unlikely by themselves to have caused the observed decreasing sea-ice trend of recent decades [*Gregory et al.*, 2002]. Simulations of HadCM3 and ECHAM4 models project, in some scenarios, an ice-free Arctic in late summer by the end of 21st century [*Gregory et al.*, 2002; *Johannessen et al.*, 2004].

[3] The complexity of physical processes involved in Arctic climate challenges CGCMs in simulating Arctic and global climate. Model defects and the paucity of observational sea-ice data make the projection of climate change in the Arctic extremely difficult and uncertain. *Rind et al.* [1995] demonstrated a large disagreement in the sensitivity of climate change to sea-ice features in climate models. *Randall et al.* [1998] found that even the large-scale dynamical aspects of Arctic climate are not well reproduced in CGCMs at that time. The *IPCC* [2001] report recently showed that present CGCMs provide wildly differing simulations of the Arctic climate. For example, there is a large

[1]Center for Ocean-Land-Atmosphere Studies, Calverton, Maryland, USA.
[2]Nansen International Environmental and Remote Sensing Center, St. Petersburg, Russia.
[3]Max-Planck-Institute for Meteorology, Hamburg, Germany.
[4]Also at Environmental Systems Science Centre, Reading, UK.
[5]Center for Atmosphere-Ocean Science, Courant Institute of Mathematical Sciences, New York University, New York, USA.


0148-0227/04/2003JD004454$09.00

**Table 1.** Sea-Ice Components of the CGCMs in the CMIP2 Integrations[a]

| Model | Output | Flux Adjustment | Sea-Ice Component |
|---|---|---|---|
| BMRC | SIT | heat, freshwater | thermodynamics |
| CCCMA | SIT | heat, freshwater | thermodynamics |
| CCSR | SIT | heat, freshwater | thermodynamics |
| CERFACS | SIT, SIC | none | thermodynamics, statistical subgridscale ice thickness distribution |
| CSIRO | SIT, SIC | heat, freshwater, momentum | thermodynamics with a cavitating fluid rheology |
| ECHAM3 | SIT | heat, freshwater, momentum | thermodynamics |
| GFDL | SIT | heat, freshwater | thermodynamics with free-drift approximation |
| GISS | SIT, SIC | none | thermodynamics |
| LMD | SIT | none | diagnostic |
| MRI | SIT, SIC | heat, freshwater | thermodynamics with free-drift approximation |
| NCAR | SIT, SIC | none | thermodynamics with a cavitating fluid rheology |
| NRL | SIT, SIC | annual mean heat, freshwater | diagnostic |
| HadCM3 | SIT, SIC | none | thermodynamics with free-drift approximation |
| HadCM2 | SIT, SIC | heat, freshwater | thermodynamics with free-drift approximation |

[a]SIC, sea-ice concentration; SIT, sea-ice thickness; BMRC, Bureau of Meteorology Research Center, Melbourne, Australia; CCCMA, Canadian Centre for Climate Modelling and Analysis, Victoria, Canada; CCSR, Center for Climate System Research, Tokyo, Japan; CERFACS, Centre European de Recherche et de Formation Avancéen en Calcul Scientifique, Toulouse, France; CSIRO, Commonwealth Scientific and Industrial Research Organization, Mordialloc, Australia; ECHAM3, Max-Planck Institute for Meteorology, Hamburg, Germany; GFDL, Geophysical Fluid Dynamics Laboratory, Princeton, New Jersey, United States; GISS, Goddard Institute for Space Studies, New York, New York, United States; LMD, Laboratoire de Metéorologie Dynamique, Institut Pierre Simon Laplace, Paris, France; MRI, Meteorological Research Institute, Tsukuba, Japan; NCAR, National Center for Atmospheric Research, Boulder, Colorado, United States; NRL, Naval Research Laboratory, Monterey, California, United States; HadCM2 and HadCM3, United Kingdom Meteorological Office, Bracknell, United Kingdom.

range in the ability of models to simulate the position of the ice edge and its seasonal cycle in the current climate. There is clear scientific merit in exploring the two-dimensional distributions of projected climate change and their disagreement in the Arctic as well as their connection to sea ice using multimodel simulations. All the CMIP2 models include comprehensive oceanic general circulation model (OGCM) and atmospheric general circulation model (AGCM) components and the simulations provide an opportunity to explore this problem, although it should be noted that some of the models were developed several years ago and do not represent present state-of-the-art models.

[4] Recently, *Holland and Bitz* [2003] documented the polar amplification of NH climate change in some models of the CMIP2 project and in the Community Climate System Model. In particular, the magnitude, spatial distribution, and seasonality of the surface warming in the Arctic were examined and compared among the models and between two groups of models with high and low polar amplification. They found that the mean sea-ice state in the control (or present) climate influences both the magnitude and spatial distribution of the high-latitude warming in the models. They also found that increases in poleward ocean heat transport at high latitudes and in polar cloud cover are significantly correlated to the amplified Arctic warming. Using some of the CMIP2 simulations, *Flato* [2004] also examined changes in the Arctic and Antarctic sea-ice climatology due to increase of greenhouse gas concentration. He found that models that produce thick ice in their unperturbed integrations exhibit less warming than those with thin ice in the Arctic.

[5] In contrast with the works of *Holland and Bitz* [2003] and *Flato* [2004], in this work, we compare and contrast all the CMIP2 model with available observations. We focus on: (1) the two-dimensional distribution of the mean and intermodel spread of Arctic sea ice and climate change at the time of $CO_2$ doubling and their interconnection; (2) the sensitivity of Arctic surface air temperature (SAT) change to sea-ice area change in different models and in various periods of forced integration of the models; (3) the possible influence of $CO_2$ doubling on sea level pressure (SLP) in high latitude; and (4) the differences resulting from model-dependent physics. In Section 2, we describe the main features of sea-ice models, and the simulated and observed data used in this study. In Section 3, the observed sea-ice climatology and the mean in the model control runs are compared. The observed sea-ice change is also briefly discussed in this Section. Section 4 shows the results of this investigation. Section 5 provides a summary and discussion of the key results.

## 2. Models: Simulated and Observed Data

[6] Simulations from the CMIP2 experiments with 14 models [*Meehl et al.*, 2000] are used in our analysis (Table 1). As Arctic climate is largely affected by the presence of sea ice, for example, the positive sea-ice albedo feedback [*Peixoto and Oort*, 1992], we list the basic features of the sea-ice component of the CMIP2 models in Table 1. In simulating sea ice, 12 of the 14 models are prognostic, while 2 models (LMD and NRL) are diagnostic (Table 1). Among the 12 prognostic models, 5 are thermodynamic-only models (BMRC, CCCMA, CCSR, ECHAM3, and GISS). The remaining 7 incorporate some kinds of sea-ice dynamics, 4 (GFDL, MRI, HadCM2, and HadCM3) use the free-drift approximation, 2 (CSIRO and NCAR) employ a cavitating fluid rheology, and CERFACS adopts a statistical subgrid-scale sea-ice thickness (SIT) distribution. Incidentally, ''free-drift'' refers to the use of an approximation in the sea-ice momentum equation which neglects the ice internal pressure. The treatments of sea-ice thermodynamics in the BMRC, CCCMA, CCSR, CSIRO, MRI, NCAR, HadCM3, and HadCM2 models are based on the two-level model of *Semtner* [1976]. Flux adjustment for surface ocean fields is applied in the BMRC, CCCMA, CCSR, CSIRO, ECHAM3, GFDL, MRI, NRL, and HadCM2 models (Table 1). Further details about the individual models can be found in *Holland and Bitz* [2003] and at http://www-pcmdi.llnl.gov/cmip/.

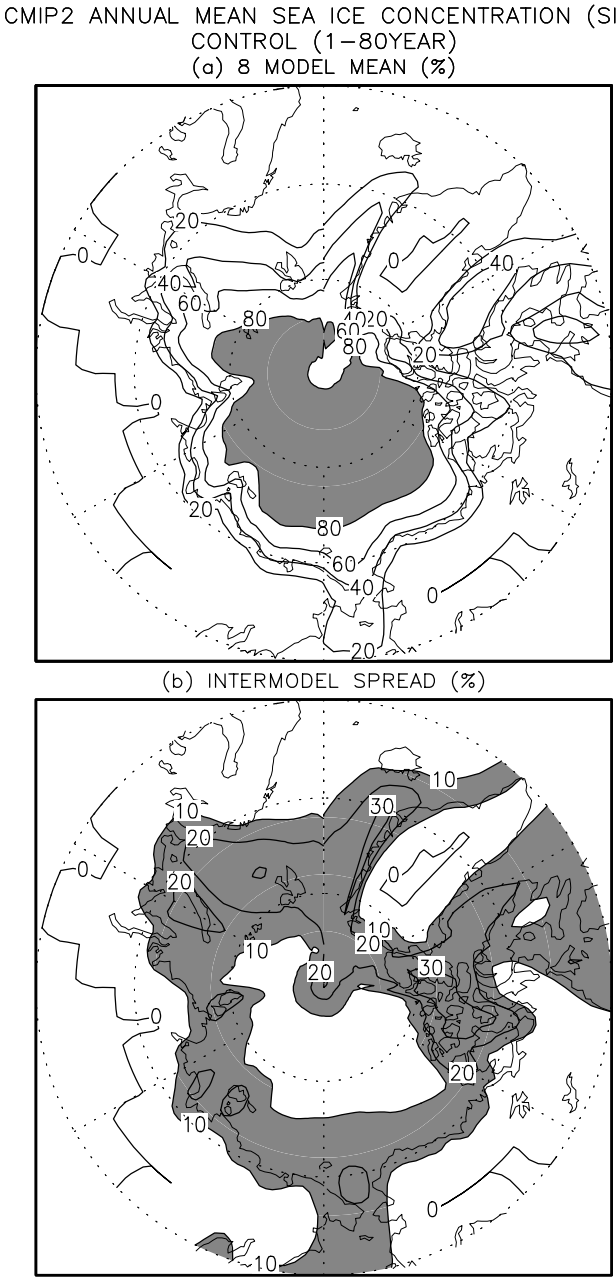


**Figure 1.** The (a) 8-model mean and (b) intermodel spread of annual SIC north of 60°N averaged for the 80 years of the control runs. The contour interval is 20% in Figure 1a and 10% in Figure 1b. Shading is used for values larger than 80% in Figure 1a and larger than 10% in Figure 1b.

[7] Each experiment consists of a control run with constant " present day" atmospheric $CO_2$ and a greenhouse-gas run with a gradual increase (i.e., 1% year$^{-1}$ compounded) in $CO_2$. Each experiment runs for 80 years, except for the NRL model which only ran for 3 years of the control run. Further details about the experiments can be found at http://www-pcmdi.llnl.gov/cmip/ or in *Räisänen* [2001]. The analysis is focused on the comparison of the 20-year means for the period of the simulated years 61–80, which centers on the $CO_2$ doubling, against the 80-year means of the control run. Among all models, 8 provided 20-year means of both sea-ice concentration (SIC) and SIT, while the remaining 6 supplied only SIT. The 8 models are CERFACS, CSIRO, GISS, MRI, NCAR, NRL, HadCM3, and HadCM2 (see Table 1). Sea-ice extent data are not available for all the CMIP2 models from the CMIP homepage (http://www-pcmdi.llnl.gov/cmip/). The 20-year annual-mean SAT, SIT, SIC, and SLP are here used to investigate the means and intermodel spreads of projected Arctic climate changes and their interconnection.

[8] Observed monthly mean SIC in the Arctic during the period 1953–1995 are used to verify the CMIP2 model simulations. The observed SIC with one-degree latitude grid square resolution were derived from various data sources, which are relatively reliable after 1953 [*Chapman and Walsh*, 1993]. In addition, we also use the annual-mean SIT averaged over 1960–1982 as an estimate of the observed SIT climatology [*Bourke and Garrett*, 1987]. The original SIT data are seasonal mean at one-degree resolution from 45.5°N to 89.5°N, digitized by Benjamin Felzer from the *Bourke and Garrett* [1987] maps of submarine sonar profiles.

## 3. Sea-Ice Climatology in the Control Runs and Observations

[9] To examine the ability of CMIP2 models to simulate the Arctic sea-ice climatology, the annual mean sea-ice climatology in the control runs is compared with the corresponding observations. The intermodel spread is defined as the root-mean-square differences among the simulations. Observed SIC differences are also presented as a reference for the projected sea-ice change due to the increase of greenhouse-gas concentrations.

[10] Figure 1a presents the annual SIC north of 60°N averaged for the 80 years of the control runs in the 8 models, in which SIC data are available (see Table 1). SIC exceeds 80% over the Arctic Ocean, which is similar to the 43-year mean of the observations shown in Figure 2a. This suggests that the models may have some ability to simulate the sea-ice climatological mean, although the models produce a somewhat reduced sea-ice area and SIC as compared with the observations. Intermodel spread is mainly located along the sea-ice edge (Figure 1b) implying large intermodel differences in simulating the edge, its seasonal extent, and retreat.

[11] The simulated SIT and intermodel spread are displayed in Figure 3. The observed annual SIT climatology is shown in Figure 4. There are obvious differences between the observations and simulations. For example, the model mean SIT maximum is in the central Arctic (Figure 3a), whereas the observed maximum is just north of the Canadian Arctic Archipelago (Figure 4). Previous numerical experiments with the NCAR model shows that the location of SIT maximum can shift dramatically as a result of seemingly small errors (comparing model atmosphere and observations) in the mean surface wind (or SLP) in a coupled climate with ice dynamics [*Weatherly et al.*, 1998]. This problem in simulating the location of the SIT maximum is relatively well known. In addition, the CMIP2 simulations produce too thick sea ice in the region from the Kara Sea to the Barents Sea. Significant differences among model simulations are also found in this region (Figure 3b).

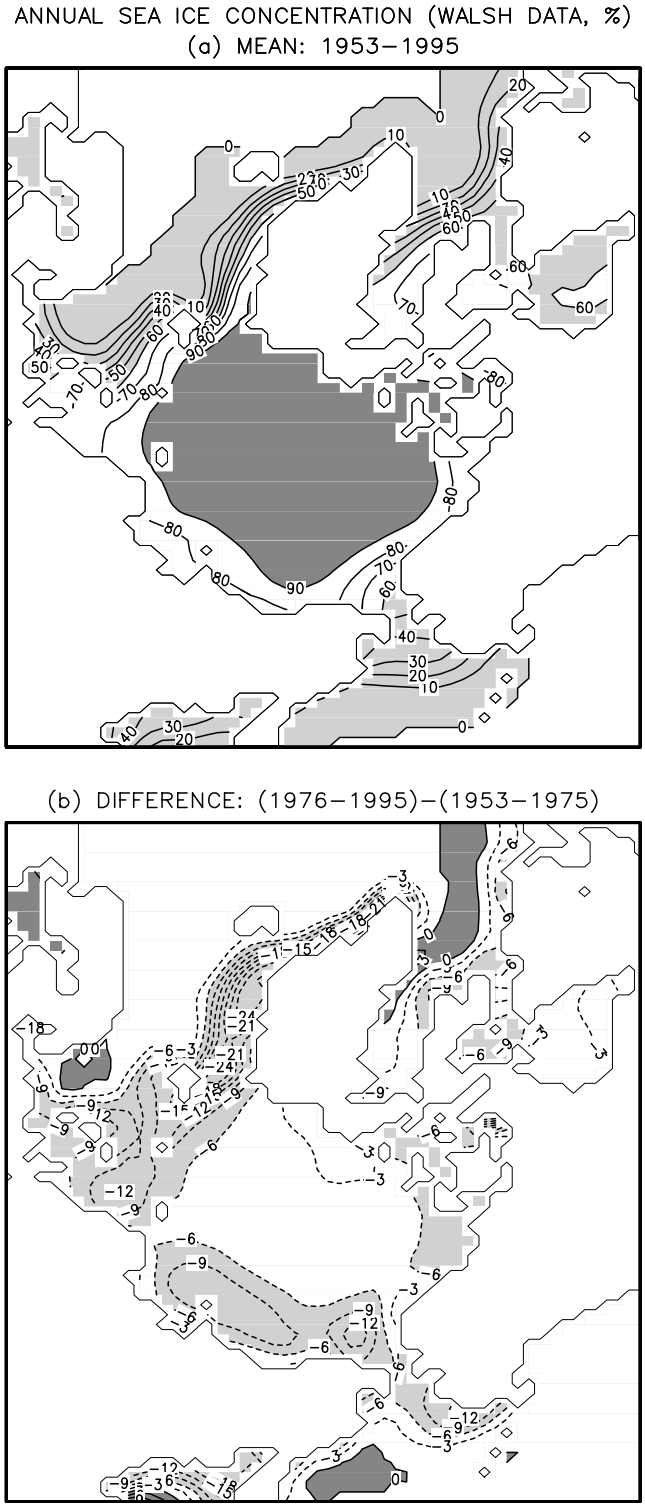


**Figure 2.** (a) Observed mean SIC in the Arctic Ocean from January 1953 to December 1995 and (b) the differences between the means of 1976–1995 and the earlier mean of 1953–1975. The contour intervals are 10% in Figure 2a and 3% in Figure 2b. Shading is used for values larger than 90% or between 10% and 60% in Figure 2a, and larger than 0% or less than −6% in Figure 2b.

Differences are also noticeable between observations and simulations around Greenland (Figures 3a and 4). It is clear that the basic features of sea-ice climatology, as simulated by individual models, needs to be further investigated.

[12] Observed SIC changes are shown as differences in Figure 2b. The most-noticeable changes are along the climatological sea-ice edge. The dominant feature is the

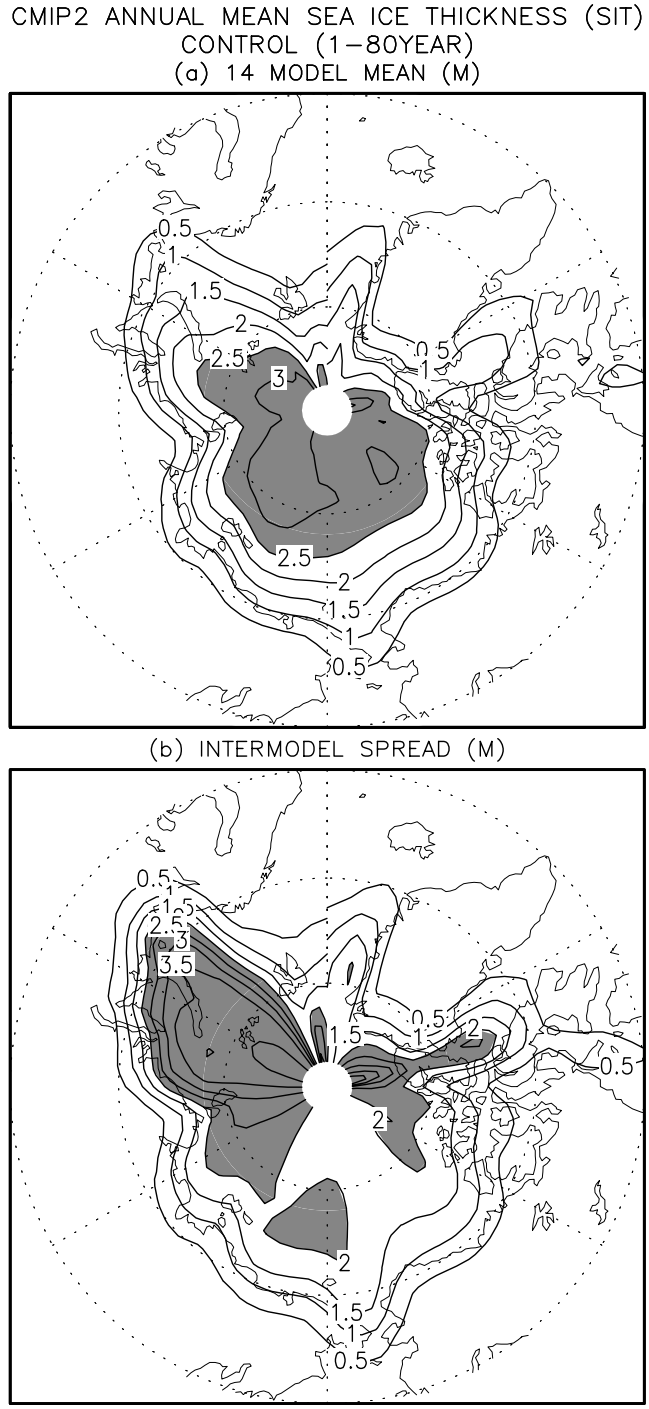


**Figure 3.** The (a) 14-model mean and (b) intermodel spread of annual SIT north of 60°N averaged for the 80 years of the control runs. The contour interval is 0.5 m. Shading represents values larger than 2.5 m in Figure 3a and larger than 2.0 m in Figure 3b.

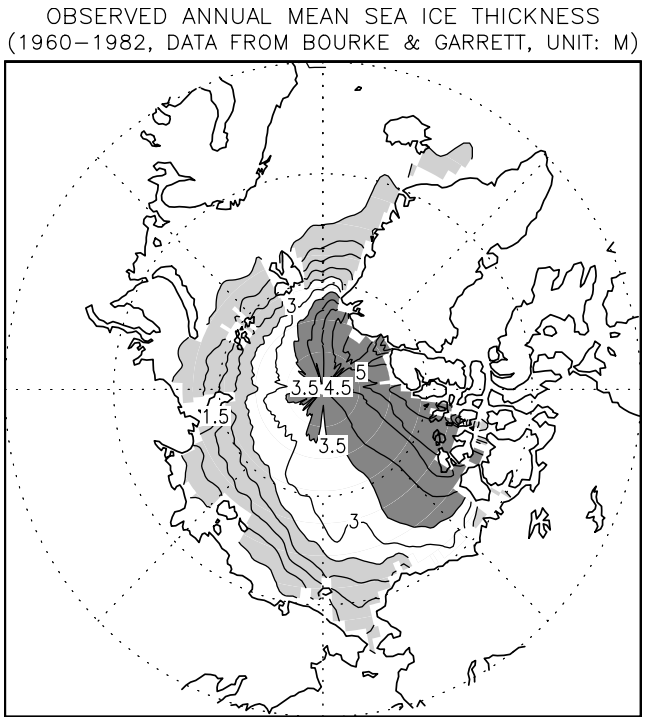


**Figure 4.** The observed annual-mean SIT climatology averaged over 1960–1982. The contour interval is 0.5 m, and dark (light) shading represents value larger than 3.5 m (between 0.5 and 2.5 m).

decrease of sea-ice area (Figure 2b). The decrease exceeds 20% along the east Greenland coast. Such features are consistent with the time series of average sea-ice extent in the NH as demonstrated in the IPCC Report (see Figures 2.14 and 2.15 in *IPCC* [2001]). *Deser et al.* [1999] found that the observed trend and first mode of natural variability of NH SIC has a dipole structure with more (less) ice to the east of Greenland when there is less (more) ice to the west of Greenland. The recent SIC trend (Figure 2b) is characterized by relatively more ice reduction on the east side of Greenland and relatively less reduction on the west side, which is similar to the patterns of standard deviation and the leading EOF mode of January–March SIC anomalies during 1958–1997 (Figures 2 and 3a of *Deser et al.* [1999]). This is also consistent with a deeper Icelandic low [*Deser et al.*, 1999]. However, it is not yet clear what role natural variability plays in these observed changes.

## 4. Simulated Sea-Ice and Climate Changes

### 4.1. SAT and Sea-Ice Changes

[13] Figure 5a shows the 14-model mean of annual Arctic SAT differences between the global-warming scenario runs in years 61–80 and the corresponding control runs. The warming near the central Arctic Ocean is more pronounced than that from the Greenland Sea to the Barents Sea. SAT increases above 4°C in the former region and below 2°C in the latter. Intermodel spread is evident, particularly over the Arctic Ocean (Figure 5b), which renders the fidelity of the overall simulated SAT change uncertain. The maximal intermodel spread is in the Barents Sea. Analysis of annual SIT change (Figure 6a) and associated intermodel spread (Figure 6b) show that SIT reduction occurs clear across the whole Arctic. The largest decrease of SIT appears mainly in the Greenland and Barents Sea region, with amplitudes of 0.3–1.8 m

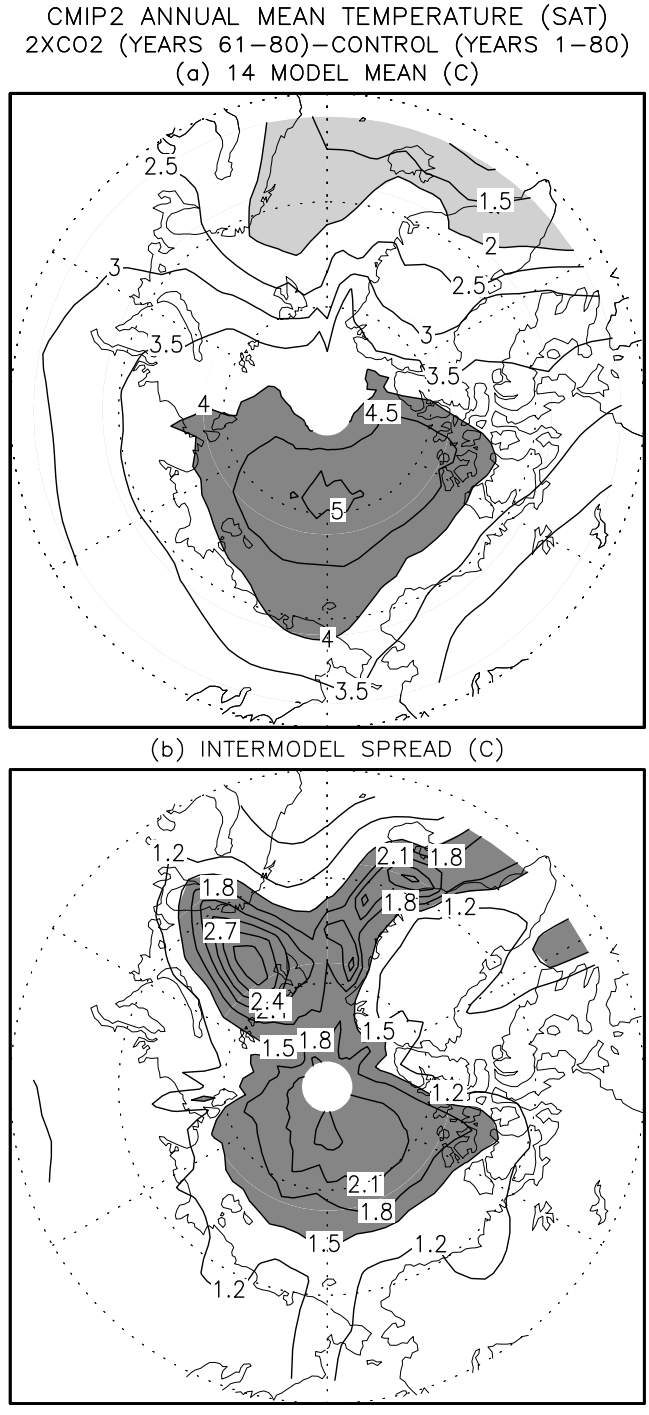


**Figure 5.** The (a) 14-model mean and (b) intermodel spread of annual SAT differences north of 60°N between $CO_2$ doubling (years 61–80) and the corresponding control runs (80 years). The contour interval is 0.5°C in Figure 5a and 0.3°C in Figure 5b. Dark (light) shading is used for values larger (less) than 4°C (2°C) in Figure 5a, and larger than 1.5°C in Figure 5b.

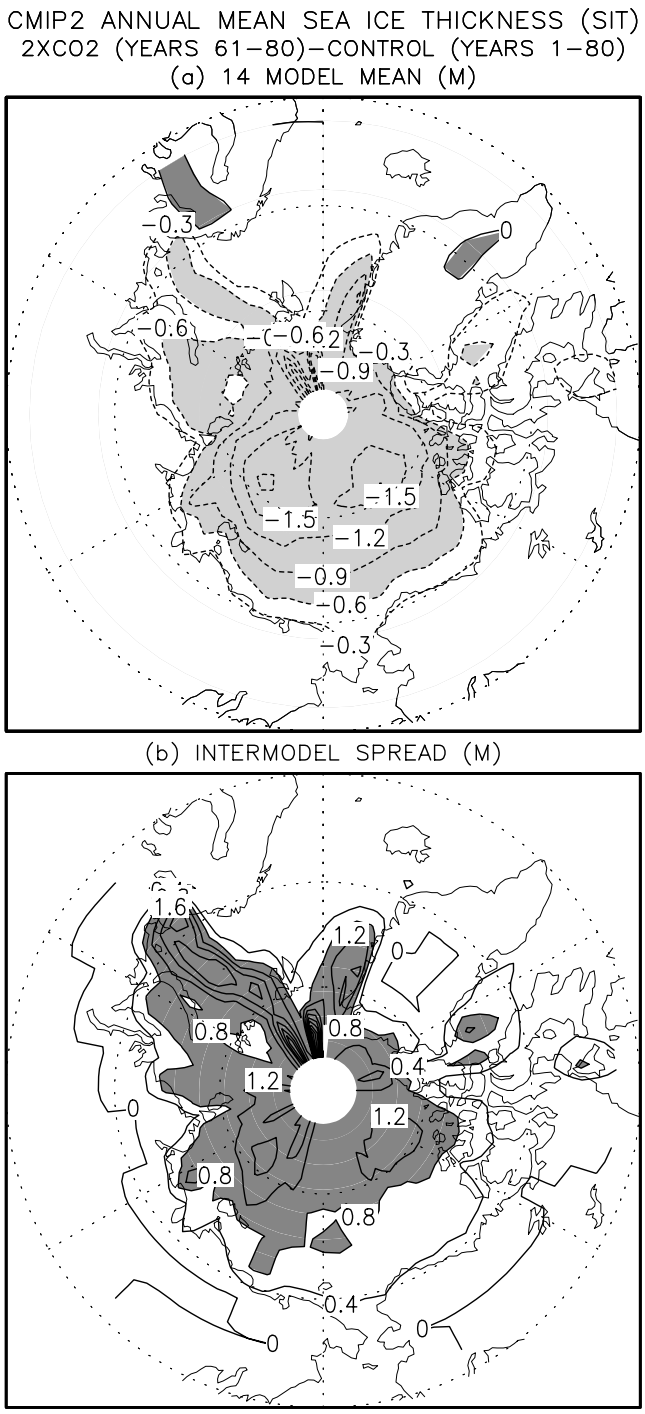


**Figure 6.** Same as in Figure 5, but for SIT. The contour interval is (a) 0.3 m and (b) 0.4 m. Shading is used for values less than −0.6 m and larger than 0.0 m in Figure 6a, and larger than 0.8 m in Figure 6b.

(Figure 6a). The largest intermodel spread exists mainly from the Barents Sea to the North Pole (Figure 6b).

[14] Comparison of Figures 5 and 6 shows a general agreement of the mean and intermodel spread patterns between the simulated SAT and SIT changes. This implies that both the mean and intermodel spread of Arctic climate change, which results from the increase in greenhouse-gas concentrations, are influenced by the interaction between sea ice and the overlying atmosphere. The intermodel spread patterns in Figures 5b and 6b are also similar to that in Figure 3b, which implies that the largest differences among the models found in the Greenland-Barents Seas are mainly due to sea-ice differences in the control runs. This is consistent with *Holland and Bitz* [2003], who found that the mean sea-ice state in the control climate greatly influences both the magnitude and spatial distribution of high-latitude warming in models. However, the role of

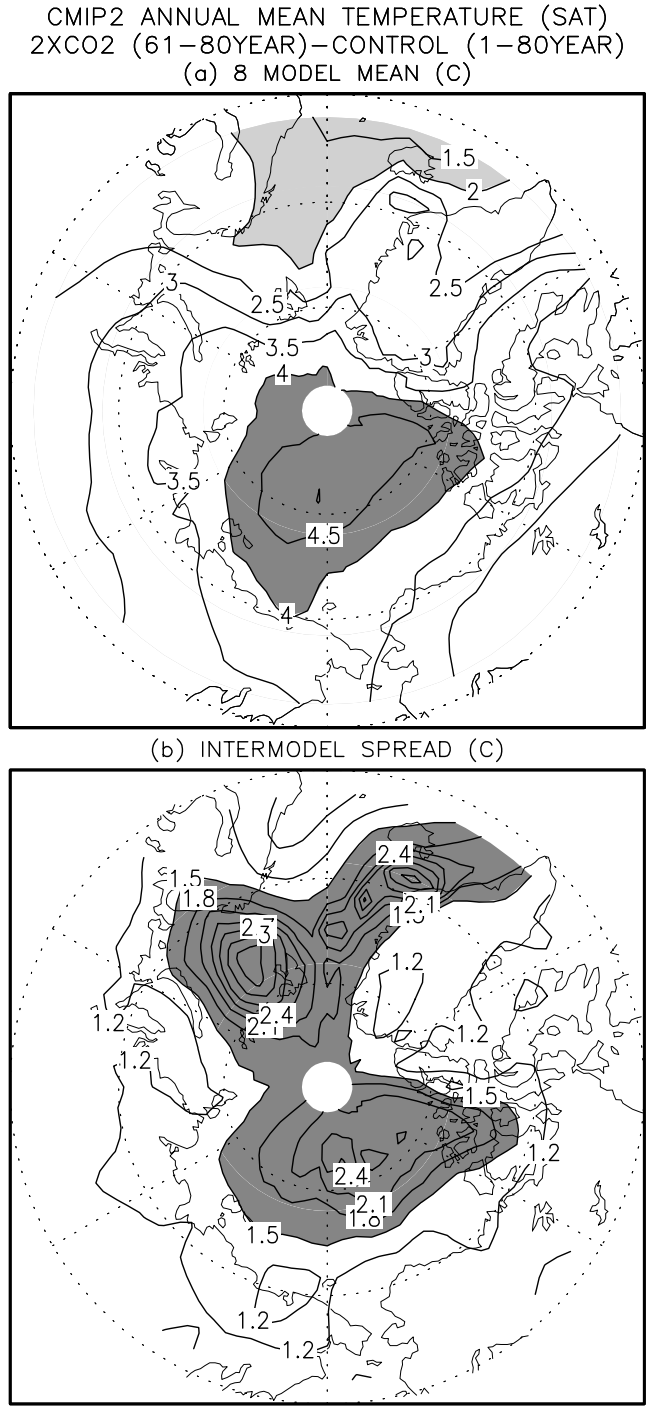


**Figure 7.** Same as Figure 5, but for SAT difference composite of the 8 models having SIC data.

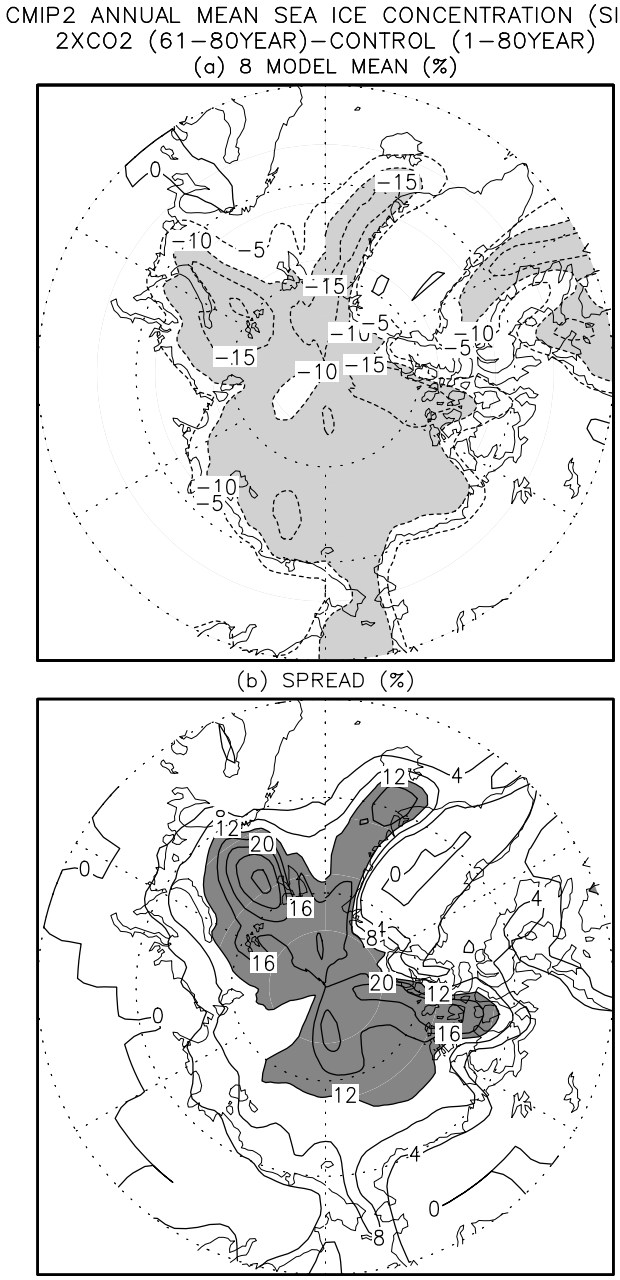


**Figure 8.** Same as Figure 6, but for the composite of SIC of the 8 models. The contour interval is (a) 5% and (b) 4%. Shading is used for values less than −10% in Figure 8a and larger than 12% in Figure 8b.

ocean heat transport and certain atmospheric processes can not be ruled out. For example, *Holland and Bitz* [2003] found that increases in poleward ocean heat transport at high latitudes and in polar cloud cover are significantly correlated to amplified Arctic warming.

[15] The agreement also exists for SAT and SIC of the 8 models (Table 1) for which the SIC data are available (Figures 7 and 8). SIC decrease over 10% in most regions of the Arctic Ocean (Figure 8a). The agreement implies that in the Arctic not only SIT but also SIC is sensitive to the increase in greenhouse-gas concentrations, and that the SAT change in the Arctic is associated with SIT change as well as SIC change. The analysis also demonstrates that the largest disagreements are mainly in Barents Seas and its vicinity in simulated SIT, SIC, and SAT, which mainly result from the differences in the control runs.

### 4.2. Sensitivity of SAT Change to Sea-Ice Area Change

[16] Both observations and model simulations show that NH sea-ice area and Arctic SAT changes are strongly connected (see Table 1 of *Bengtsson et al.* [2004]). The sensitivity of Arctic SAT to sea-ice change becomes a measure to compare the behavior among models, as well as between models and observations. The sensitivity, defined as the ratio of annual Arctic SAT change to NH annual sea-ice area change [*Bengtsson et al.*, 2004], is shown in Figure 9a. The Arctic SAT and the NH sea-ice area changes are the differences between the mean in a specified period of the greenhouse-gas forced runs and the mean in the 80-year control runs. The Arctic SAT is the average northward of 60°N and the NH sea-ice area is converted from the SIC data. The values of the sensitivity range from −2.5 to 1.5°C/$10^6$ km$^2$. Almost all models show a negative sensitivity with values hovering close to −1.5°C/$10^6$ km$^2$. The only exception exception is the MRI model, it gives a positive sensitivity in the first 20 years of the forced run.

[17] These sensitivity findings are consistent with the calculations of *Bengtsson et al.* [2004] using both observational data and model simulations. The observed sensitivity values are −0.98°C/$10^6$ km$^2$ using the observed data for 1953–1998 of *Chapman and Walsh* [1993], and −1.44°C/$10^6$ km$^2$ using the 1900–1993 observations of *Zakharov* [1997] [see *Bengtsson et al.*, 2004]. The averaged sensitivity value in the ECHAM model simulations, forced with observed SST and SIC, is −0.91°C/$10^6$ km$^2$ (Table 1 of *Bengtsson et al.* [2004]). However, our calculations show that sensitivity is different in different models, and even within various periods of a particular model. In the discussion that follows, largest (smallest) sensitivity means largest (smallest) amplitude of negative values. The NCAR model has the highest sensitivity while the MRI model shows the lowest, with the sensitivity of the former about four times that of the latter.

[18] One possibility is that the sensitivity differences among models may be explained by the differences in poleward ocean heat transport in the models. *Holland and Bitz* [2003, Figure 8a] show that among 8 analyzed CMIP2 models within the latitude band 60°N to 90°N, the MRI model has strongest poleward ocean heat transport change and the NCAR model the weakest. Stronger poleward ocean heat transport brings more warm water from low latitudes to high latitudes, which favors melting more sea ice. The averaged SAT in NH does not change much, since the heat transport just moves the warm water from one place to another in NH. That weakens the regional connection between SAT and sea-ice area changes and leads to a smaller sensitivity. Two caveats in interpreting these intercomparison results are: first, we note that the MRI model has the largest sensitivity divergence among the models (Figure 9a), and secondly, when using 20-year means to calculate the sensitivity, some natural variability in SAT and sea-ice area are involved.

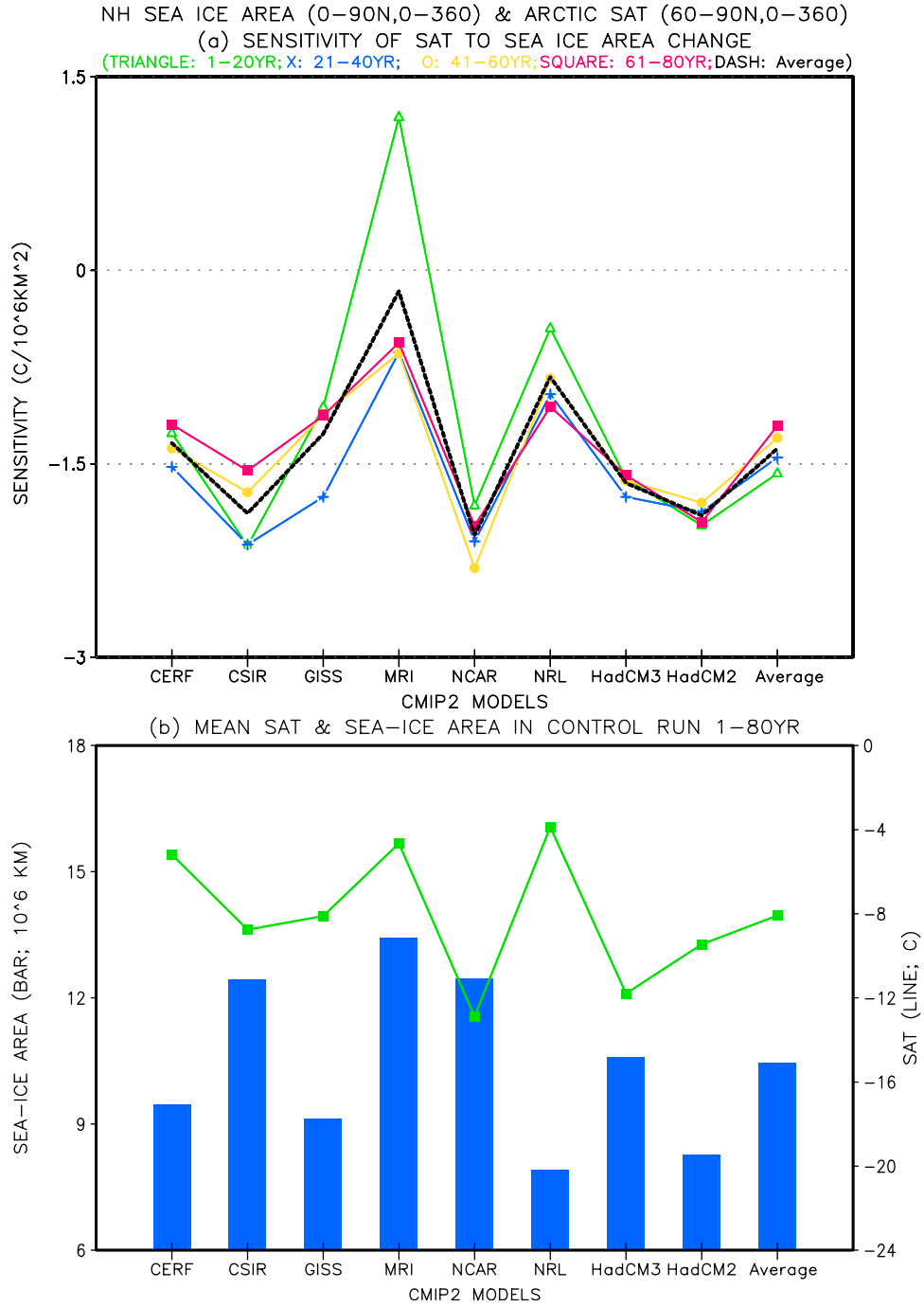


**Figure 9.** (a) Sensitivity of models in different periods of the greenhouse-gas forced integration, and (b) mean SAT (line) and sea-ice area (bar) in the 80-year control runs. In Figure 9a, the curves with triangle, cross, circle, and square represent the sensitivity calculated by comparing the mean Arctic SAT and NH sea-ice area averaged over years 1–20, 21–40, 41–60, and 61–80 of the forced runs with the corresponding means of 80 year control runs, respectively. The dashed line in Figure 9a is the mean value for individual model. The 8-model mean is shown as the last value of each plot.

[19] In order to explore the influence of initial SAT and sea-ice area on the sensitivity, the mean SAT and sea-ice area in the control runs are displayed (Figure 9b). Comparing the sensitivities (Figure 9a) with the corresponding mean sea-ice area in the 80-year control runs, we do not find any connection between the sea-ice area in the control run and the sensitivity. However, the comparison shows a possible connection between the mean SAT and the sensitivity. A warmer (colder) Arctic climate in a model is generally related with a lower (higher) sensitivity, although the relationship is not linear and an obvious underlying mechanism is unclear.

[20] If the mean of the control run is replaced by the mean of the first 20 years of the forced run as a reference

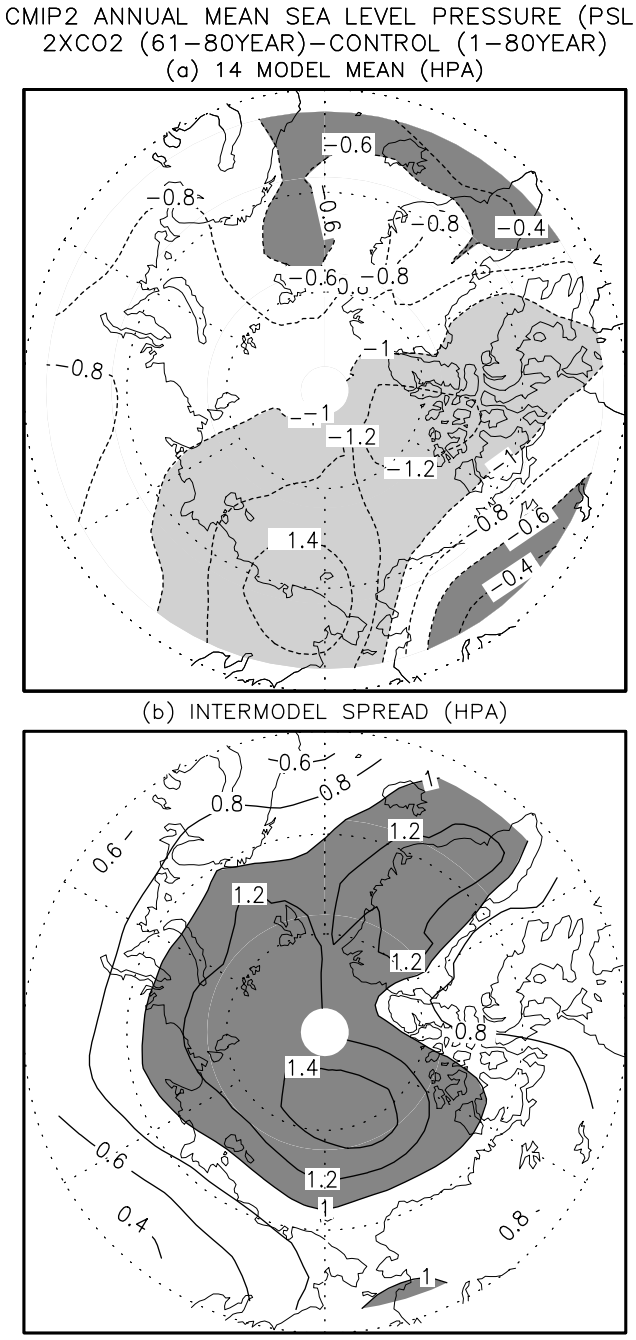


**Figure 10.** Same as Figure 5, but for SLP. The contour interval is 0.2 hPa. Shading is used for (a) values less than −1.0 hPa or greater than −0.6 hPa and (b) values larger than 1.0 hPa.

period in calculating the sensitivity, the conclusions about the sensitivity and the relation between SAT and sensitivity are generally the same, except for the period 21–40 years of the CERFACS and GISS models. The reason is that SAT is almost without increase in the CERFACS model when compared to a reasonable sea-ice area decrease. The GISS model even produces a sea-ice area increase from the period 1–20 years to that of 21–40 years.

[21] The MRI and NRL models are outliers in Figures 9a and 9b. The MRI model simulated the largest sea-ice area and the NRL model produced the smallest. These two models also have the lowest sensitivity. Composites excluding these two models indicate that the patterns of SAT, SIT, and SLP (not shown) are almost identical to the corresponding ones in Figures 5, 6, and 10, except for some amplitude differences.

### 4.3. Projected SLP Change

[22] Figure 10 exhibits the mean and intermodel spread of the annual SLP change of the 14 models. The patterns in Figure 10 are generally consistent with those in Figures 5–8. A large (small) decrease of SLP (Figure 10a) coexists with a large (small) increase of SAT (Figures 5a and 7a), and a large (small) reduction of SIT and SIC (Figures 6a and 8a). Major intermodel spreads are mainly confined to the Arctic Ocean in all the simulations (Figures 5–8 and 10). Those similarities suggest that the mean and intermodel spread of the climate response in the Arctic are influenced by local sea-ice - atmosphere interaction. This is consistent with the results of *Semenov and Bengtsson* [2003], who found that observed low-frequency variation of Arctic SAT is associated with long-term sea-ice variability in the Kara-Barents Seas and Baffin Bay.

[23] The decrease in the mean SLP response is larger in higher latitudes than in lower latitudes (Figure 10a), which results in the enhancement of north-south SLP gradient and the mean westerly winds. This agrees with the analysis of *Hu and Wu* [2004] and *Kuzmina et al.* [2004], who found a north-south SLP gradient intensification due to the increase of greenhouse-gas concentrations. It is interesting to note that the intermodel spread pattern of SLP (Figure 10b) shows some similarities to the trend-noise pattern of 500 hPa geopotential height (see Figure 2a in *Schneider et al.* [2003]). The trend-noise pattern is defined as the root-mean-square amplitude of intra-ensemble variability of 500 hPa geopotential height trends in the NH winter from an ensemble produced from a T63 atmospheric general circulation model. This may imply that internal dynamics in the Arctic are important in predicting climate change.

### 4.4. Differences Resulting From Model Physics

[24] There is a tendency for models not employing flux adjustment (CERFACS, GISS, NCAR, and HadCM3) to have relatively larger temperature sensitivity to SIC changes than models using flux adjustment (Figure 9a). Figure 11 shows the differences of SAT response to the increase in greenhouse gas concentrations between the models with and without flux adjustment. The general patterns of temperature changes are similar for the models with and without flux adjustment, although the amplitudes are slightly smaller in the former than in the latter, particularly in the Barents and Kara Seas (Figures 11a and 11c). The amplitude differences are mainly due to the extremely small temperature change simulated by the NRL model (not shown).

[25] The intermodel spread in models without flux adjustment (Figure 11d) is smaller than in the models with flux adjustment (Figure 11b) in most regions of the Arctic Ocean, except for the region from the Barents and

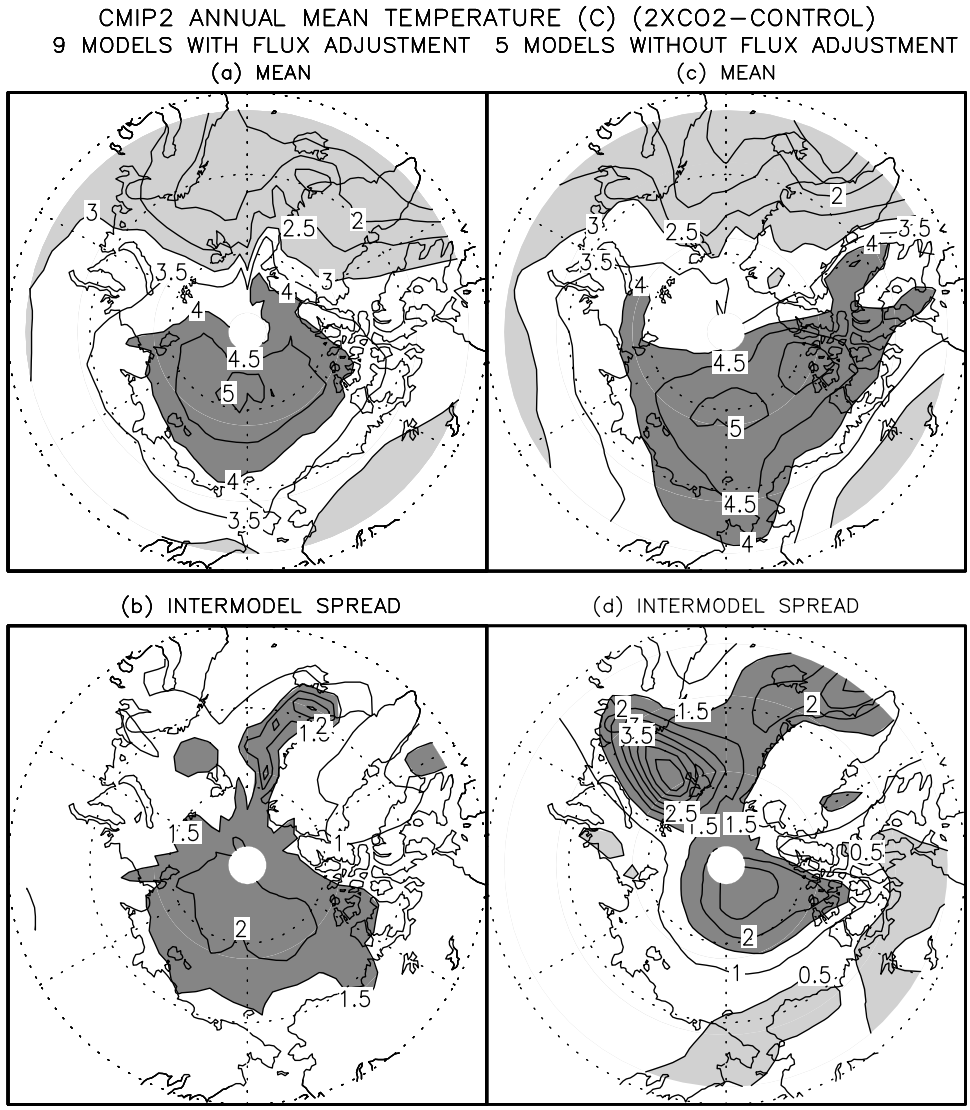


**Figure 11.** Annual SAT differences north of 60°N between $CO_2$ doubling and the control runs. (a) and (b) Mean and intermodel spread of the 9 models which employ flux adjustment; (c) and (d) mean and intermodel spread of the 5 models which do not use flux adjustment. The contour interval is 0.5°C. Shaded regions represent values larger than 4.0°C or less than 3.0°C in Figures 11a and 11c, and larger than 1.5°C or less than 0.5°C in Figures 11b and 11d.

Kara Seas to the North Pole. The larger intermodel spread in the region from the Barents and Kara Seas to the North Pole in the models without flux adjustment is mainly caused by opposing patterns simulated by the GISS and LMD models: the GISS model produces a tremendous cooling and the LMD model gives a large warming from the Barents Sea to the North Pole (not shown). It is not clear what are the reasons underlying the substantive differences between the two models.

[26] The role of sea-ice dynamics in high-latitude climate has been demonstrated in many investigations. For example, *Vavrus and Harrison* [2003] found that sea-ice dynamics produces cooler anomalies than simulations without dynamics, resulting in reduced Arctic warming in warm scenarios and increased cooling in cold scenarios. *Holland et al.* [1993] indicated that models that include dynamical sea-ice processes tend to be less sensitive to changes in forcing, at least with regard to SIC. It has been suggested that sea-ice dynamics provides various negative feedbacks to the air-ice-ocean systems. However, we do not find significant or consistent differences in the sensitivity of SAT change to sea-ice change between the mean simulations with and without sea-ice dynamics. This agrees with the conclusion of *Flato* [2004], who concluded that intermodel differences in sea-ice state and the sea-ice response to climate forcing are determined more by feedbacks involving the atmosphere and ocean than by attributes of the sea-ice component. Using multimodel means we are led to the conclusion that these negative feedbacks are not important. We caution that this is a preliminary finding, and may be misleading as the behavior of some individual model may conceal the differences between the means of the models with and without sea-ice

dynamics. Future CMIP-type experiments will help elucidate this point.

## 5. Summary and Discussion

[27] In this study, we have investigated the Arctic sea-ice simulations of the CMIP2 models and analyzed their spatial distribution of sea-ice and climate changes at the time of $CO_2$ doubling. We also investigated to what extent coupling between the atmosphere and sea-ice can be responsible for the spread in climate sensitivity as simulated by individual CMIP2 models. We further explored the sensitivity of temperature change to sea-ice area change and the possible influence of the nature of the sea-ice component model on the simulated climate change.

[28] Comparison with observations shows that in their control runs the mean of the CMIP2 models simulates the basic features of the observed sea-ice climatology reasonably well. A noticeable deficiency in mean-model simulations is that they produce too thick sea ice compared with observations in the regions from the Kara Sea to the Barents Sea. In the global warming scenario simulations, warming from the Chukchi Sea to the East Siberian Sea is more pronounced than that from the Greenland Sea to the Barents Sea. SAT increases above 5°C in the former regions and below 1°C in the latter. The intermodel spread is pronounced, particularly in the Arctic Ocean, with a maxima in the Barents Sea. SIT change appears mainly in the Greenland-Barents Seas with the reduction ranging from 0.3 to 1.8 m. The largest intermodel spread exists from the Barents Sea to the North Pole. SIC decrease more than 10% in most regions of the Arctic Ocean. The sensitivity of Arctic SAT change with respect to sea-ice area change is model dependent. For some models, the sensitivity is different even during different periods of the transient integration. The values of sensitivity lie in the range $-2.0$ to $-0.5$°C/$10^6$ km$^2$ for most models. Colder (warmer) Arctic climate may favor higher (lower) sensitivity.

[29] The simulated mean and intermodel spread patterns of SAT change are similar to those of SIT and SLP changes, implying that the mean and intermodel spread of projected Arctic climate change are influenced by the interaction between sea-ice and the atmosphere. Both SIT and SIC are sensitive to the increase in greenhouse-gas concentrations, and are connected with SAT and SLP changes in the Arctic. On average, for all model simulations, the north-south SLP gradient and the mean westerly winds are enhanced at the time of $CO_2$ doubling. Both the mean and intermodel spread patterns show considerable differences between models with and without flux adjustment in some regions. The detailed physical processes and responsible mechanisms clearly need to be better understood than at present, but this is not an easy task given the overwhelming complexity of the models.

[30] It should be mentioned that due to the small number of model simulations, the statistical significance of the differences is not discussed. Further numerical experiments are needed in order to test such significance and to understand the mechanisms behind the differences. However, assuming that the mean represents signal and the intermodel spread is noise, then the above analysis allows for the conclusion that there is still high disagreement in the simulated climate and sea-ice changes in the Arctic region resulting from an increase in greenhouse-gas concentrations in the CMIP2 runs. Even for the mean climate in the control runs, differences among individual models are large (not shown). The disagreement in the simulated Arctic climate change may be one of the important factors affecting global climate projection. In order to give a better simulation for the Arctic sea ice and climate, it is also necessary to improve the parameterization of physical processes in both atmospheric and oceanic component models, as suggested by *Randall et al.* [1998], since sea-ice errors in simulations result not only from the sea-ice component itself, but also from other aspects of a climate model (i.e., atmosphere and ocean), as discussed by *Flato* [2004]. Further study using sensitivity simulations within a single model is also necessary to investigate the mechanisms behind the results presented here.

[31] **Acknowledgments.** The authors thank the editor A. Robock and anonymous reviewers for their suggestions and comments to significantly improve the manuscript. The authors thank E. Schneider, R. Stouffer, B. Huang, and D. Straus for their discussion and suggestions, and also B. Wu and J. Adams for their assistance in processing the observed sea-ice data. This work was supported by a grant from the U.S. Department of Energy (DE-FG02-01ER63256). D.M.H. acknowledges support from the Office of Polar Programs of the National Science Foundation grants OPP-9901039 and OPP-0084286. All CMIP2 modeling groups are acknowledged for making the simulations available. CMIP2 model data are provided by the Program for Climate Model Diagnosis and Intercomparison (PCMDI) at the Lawrence Livermore National Laboratory (LLNL).

## References

Bengtsson, L., V. A. Semenov, and O. Johannessen (2004), The early century warming in the Arctic—A possible mechanism, *J. Clim*, in press.

Bourke, R. H., and R. P. Garrett (1987), Sea ice thickness distribution in the Arctic Ocean, *Cold Reg. Sci. Technol.*, *13*, 259–280.

Chapman, W., and J. Walsh (1993), Recent variations of sea ice and air temperature in high latitudes, *Bull. Am. Meteorol. Soc.*, *74*, 33–47.

Deser, C., J. E. Walsh, and M. S. Timlin (1999), Arctic sea ice variability in the context of recent atmospheric circulation trends, *J. Clim.*, *13*, 617–633.

Flato, G. M. (2004), Sea ice and its response to $CO_2$ forcing as simulated by several global climate models, *Clim. Dyn.*, in press.

Gregory, J. M., P. A. Stott, D. J. Cresswell, N. A. Rayner, C. Gordon, and D. M. H. Sexton (2002), Recent and future changes in Arctic sea ice simulated by the HadCM3 AOGCM, *Geophys. Res. Lett.*, *29*(24), 2175, doi:10.1029/2001GL014575.

Holland, D. M., L. A. Mysak, D. K. Manak, and J. M. Oberhuber (1993), A sensitivity study of a dynamic-thermodynamic sea-ice model, *J. Geophys. Res.*, *98*, 2561–2586.

Holland, M. M., and C. M. Bitz (2003), Polar amplification of climate change in coupled models, *Clim Dyn.*, *21*, 221–232.

Hu, Z.-Z., and Z. Wu (2004), The intensification and shift of the annual North Atlantic Oscillation in a global warming scenario simulation, *Tellus, Ser. A*, *64*(2), 112–124.

Intergovernmental Panel on Climate Change (IPCC) (2001), *Climate Change 2001: The Scientific Basis—Contribution of Working Group I to the Third Assessment Report of the Intergovernment Panel on Climate Change*, edited by J. T. Houghton et al., 881 pp., Cambridge Univ. Press, New York.

Johannessen, O. M., M. W. Miles, and E. Bjorgo (1995), The Arctic's shrinking sea ice, *Nature*, *376*, 126–127.

Johannessen, O. M., E. V. Shalina, and M. W. Miles (1999), Satellite evidence for an Arctic sea ice cover in transformation, *Science*, *286*, 1937–1939.

Johannessen, O. M., et al. (2004), Arctic climate change—Observed and modeled temperature and sea ice variability, *Tellus*, in press.

Kuzmina, S. I., O. M. Johannessen, L. Bengtsson, L. P. Bobylev, and O. G. Aniskina (2004), The North Atlantic Oscillation variability and change under anthropogenic forcing, *Tellus*, in press.

Meehl, G. A., G. J. Boer, C. Covey, M. Latif, and R. J. Stouffer (2000), The Coupled Model Intercomparison Project (CMIP), *Bull. Am. Meteorol. Soc.*, *81*, 313–318.

Peixoto, J. P., and A. H. Oort (1992), *Physics of Climate*, 520 pp., Springer-Verlag, New York.

Räisänen, J. (2001), $CO_2$-induced climate change in CMIP2 experiments: Quantification of agreement and role of internal variability, *J. Clim.*, *14*, 2088–2104.

Randall, D., J. Curry, D. Battisti, G. Flato, R. Grumbine, S. Hakkinen, D. Martinson, R. Preller, J. Walsh, and J. Weatherly (1998), Status of and outlook for large-scale modeling of atmosphere-ice-ocean interactions in the Arctic, *Bull. Am. Meteorol. Soc.*, *79*, 197–219.

Rayner, N. A., E. B. Horton, D. E. Parker, C. K. Folland, and R. B. Hackett (1996), Version 2.2 of the global sea-ice and sea surface temperature data set, 1903–1994, *Clim. Res. Tech. Note 74*, Hadley Centre, Devon, UK.

Rind, D., R. Healy, C. Parkinson, and D. Martinson (1995), The role of sea ice in $2xCO_2$ climate model sensitivity. Part I: The total influence of sea ice thickness and extent, *J. Clim.*, *8*, 449–463.

Rothrock, D. A., Y. Yu, and G. A. Mayhut (1999), Thinning of the Arctic sea-ice cover, *Geophys. Res. Lett.*, *26*, 3469–3472.

Schneider, E. K., L. Bengtsson, and Z.-Z. Hu (2003), Forcing of Northern Hemisphere climate trends, *J. Atmos. Sci.*, *60*, 1504–1521.

Semenov, V. A., and L. Bengtsson (2003), Modes of the wintertime Arctic temperature variability, *Geophys. Res. Lett.*, *30*(15), 1781, doi:10.1029/2003GL017112.

Semtner, A. J., Jr. (1976), A model for the thermodynamic growth of sea ice in numerical simulations of climate, *J. Phys. Oceanogr.*, *6*, 379–389.

Vavrus, S., and S. P. Harrison (2003), The impact of sea-ice dynamics on the Arctic climate system, *Clim. Dyn.*, *20*, 741–757.

Vinnikov, K. Y., A. Robock, R. J. Stouffer, J. E. Walsh, C. L. Parkinson, D. J. Cavalieri, J. F. B. Mitchell, D. Garrett, and V. F. Zakharov (1999), Global warming and Northern Hemisphere sea ice extent, *Science*, *286*, 1934–1937.

Weatherly, J. W., B. P. Briegleb, W. G. Large, and J. A. Maslanik (1998), Sea ice and polar climate in the NCAR CSM, *J. Clim.*, *11*, 1472–1486.

Zakharov, V. F. (1997), Sea ice in the climate system, *WMO/TD 782*, 80 pp., World Clim. Res. Programme/Arctic Clim. Syst. Study, Geneva.

L. Bengtsson, Max-Planck-Institute for Meteorology, Bundesstrasse 55, D-20146 Hamburg, Germany.

D. M. Holland, Center for Atmosphere-Ocean Science, Courant Institute of Mathematical Sciences, New York University, 251 Mercer Street, New York, NY 10012, USA.

Z.-Z. Hu, Center for Ocean-Land-Atmosphere Studies, 4041 Powder Mill Road, Suite 302, Calverton, MD 20705, USA. (hu@cola.iges.org)

S. I. Kuzmina, Nansen International Environmental and Remote Sensing Center, Bolshaya Monetnaya Street, 26/28, 197101 St. Petersburg, Russia.